Properties of Single Cardiac Na Channels at 35°C

K. BENNDORF

From the Department of Physiology, University of Cologne, 50931 Cologne, Germany

ABSTRACT Single Na channel currents were recorded in cell-attached patches of mouse ventricular myocytes with an improved patch clamp technique. Using patch pipettes with a pore diameter in the range of 200 nm, seals with a resistance of up to 4 TΩ were obtained. Under those conditions, total noise could be reduced to levels as low as 0.590 pA rms at 20 kHz band width. At this band width, properties of single-channel Na currents were studied at 35°C. Six out of a total of 23 patches with teraohm seals contained channel activity and five of these patches contained one and only one active channel. Amplitude histograms excluding transition points showed heterogenous distributions of levels. In one patch, part of the openings was approximately Gaussian distributed at different potentials yielding a slope conductance of 27 pS. The respective peak open probability at −10 mV was 0.26. The mean open time was determined at voltages between −60 and −10 mV by evaluation of the distribution of the event-related gaps in the center of the baseline noise to be ~40 μs at −60 mV and 50–74 μs between −50 and −10 mV. It is concluded that single cardiac Na channels open at 35°C frequently with multiple levels and with open times in the range of several tens of microseconds.

INTRODUCTION

Development of efficient techniques for both cell isolation and voltage clamp allowed measurement of Na currents in individual mammalian cells including those of the heart (Lee, Weeks, Kao, Akaike, and Brown, 1979; Brown, Lee, and Powell, 1981; Bustamante, 1983; Benndorf, Boldt, and Nilius, 1985). The fast kinetics of these currents already at room temperature and the limited speed in the whole cell voltage clamp, however, led most investigators to study properties of Na currents in mammalian cells at unphysiologically low temperatures. Only few data of macroscopic Na currents near the body temperature of mammals have been reported. These include cell clusters of chick embryonic heart cells (Ebihara, Shigeto, Lieberman, and Johnson, 1980) and single whole cells (myocardial mouse cells [Benndorf and Nilius, 1987], myoballs derived from human skeletal muscle [Pröbstle, Rüdel, and Ruppersberg, 1988]). Improved resolution of Na current kinetics at 37°C has been reported by Murray, Takafumi, Bennett, and Hondeghem, (1990) in large patches generating macroscopic currents. All these data show that in this tempera-

Address correspondence to K. Benndorf, Department of Physiology, University of Cologne, Robert Koch Strasse 39, 50931 Cologne, Germany.

J. GEN. PHYSIOL. © The Rockefeller University Press · 0022-1295/94/11/0801/20 $2.00
Volume 104 November 1994 801–820

ture range, Na currents decay in the positive slope region of the current-voltage characteristic within hundreds of microseconds and activate even faster.

Recording of currents through single Na channels has been more limited by the signal-to-noise ratio which excluded kinetic analysis at the body temperature of mammals. In the past, the cut-off frequency could not be increased to beyond 5 kHz. Therefore, single-channel analysis has been performed only at room temperature or below (Cachelin, DePeyer, Kokubun, and Reuter, 1983; Horn and Vandenberg, 1984; Vandenberg and Horn, 1984; Scanley and Fozzard, 1987). Recently, the use of amplifiers with integrating headstages and improvements of the recording technique (Levis and Rae, 1993; Benndorf, 1993) allowed substantial elevation of the band width. With such a technique, Benndorf and Koopmann (1993) studied properties of single cardiac Na channels at room temperature at a band width of up to 20 kHz.

In the present study, a strategy is described which was successful in further reducing the total noise in cell-attached patches. The main improvement comes from the use of unusually thick-walled pipettes and a considerable reduction of the patch area which allowed us to work with seals in the range of teraohms. The quality of the recordings was sufficient to study the action of single cardiac Na channels at 35°C.

MATERIALS AND METHODS

Cell Isolation and Solutions

Mouse ventricular myocytes were isolated by enzymatic digestion as described previously (Benndorf, 1993). Before starting the measurements, the cells were incubated for at least 15 min in the hypertonic and depolarizing bath solution which contained (in millimoles/liter) KCl, 250.0; CsCl, 20.0; $MgCl_2$, 5.0; EGTA 10.0; HEPES, 5.0; pH 7.3 with KOH. The pipette solution was composed of (in millimoles/liter) NaCl, 255.0; $CaCl_2$, 2.5; $MgCl_2$, 1.0; KCl, 4.0; HEPES, 5.0; nitrendipine, 0.002; pH 7.3 with NaOH. Solutions were made hypertonic to enlarge the single-channel current amplitude (Yue, Lawrence, and Marban, 1989).

Experimental Chamber

The experimental chamber was mounted on the stage of an inverted microscope. The chamber assembly was composed of a flat brass block in which a thin-walled (0.4 mm) plexiglass vessel with glass bottom was inserted. The temperature of the metal block was controlled by a thermostat. Immediately before starting the measurements, the fluid level was decreased to 200–300 μm. The temperature was measured in the bath with a small sensor positioned at a distance of ~ 1 mm from the tip of the patch pipette. The temperature in all measurements was 35 ± 0.3°C.

Recording Technique

Measurements were performed with a patch clamp technique (Hamill, Marty, Neher, Sakmann, and Sigworth, 1981) with improved resolution using very short pipettes (total length, 8 mm) in combination with a special tipped holder. The technique has been described in detail previously (Benndorf, 1993). Currents were recorded in cell-attached patches with high-ohmic pipettes (50–90 MΩ when filled with the hypertonic pipette solution) yielding a typical seal resistance between 1,000 and 4,000 GΩ (1–4 TΩ; for fabrication and properties of the pipettes, see below). Recording was performed with an Axopatch 200A amplifier (integrating headstage, Axon Instruments, Inc., Foster City, CA) which had an intrinsic noise of 0.416 pA rms (20 kHz,

8-pole-Bessel filter, Frequency Devices, Inc., Haverhill, MA). Patches were pulsed at a rate of 20 Hz. Capacitive transients were compensated for on line by the use of four exponentials. Remaining capacitive and leak currents were removed by subtraction of a sliding averaged blank formed from 10 empty traces out of the neighborhood of the actual record. Single Na channel currents were identified by their large amplitudes and the fast time course of the mean current. L-type Ca channels were blocked by nitrendipine.

Fabrication of High-Ohmic Patch Pipettes

The patch pipettes were pulled by a three-stage pull from thick-walled borosilicate glass tubes with an external diameter of 2.0 mm and an internal diameter of 0.5 mm. The pipettes were coated with Sylgard 184® as close as possible to the tip (~40 μm) and were not fire polished because the tips were too small to allow for optical control of the polishing process. Filling of the pipettes, 40 mm long at this stage, was performed only via the back end to avoid any contamination of the tiny pore. The filling procedure consisted of four steps. (*a*) Via a plastic tube, pulled out in the heat to a ~300-μm outer diameter, the pipette solution was injected as close to the tip as possible. (*b*) Waiting for 1 to 2 min caused filling of the pipette tips, leaving, however, a large air bubble in the conical shank (as controlled by a stereo microscope). (*c*) The pipette was connected by a short silicon tube to a 20-ml syringe with which a maximal vacuum was administered thereby enlarging the air bubble. The pipette was then hit vigorously with the finger, holding the tip downward. This caused the formation of numerous smaller air bubbles, some being small enough to migrate upward. In proportion to the relief of the vacuum, the size of the bubbles decreased and further bubbles were able to migrate upward. Repeating this procedure several times left regularly only one small bubble in the pipette which could not be removed. (*d*) Waiting for another couple of minutes caused dissolution of this bubble. After finishing, the pipette was shortened to its final length of 8 mm by first sawing it with a file and then breaking it while the front part was fixed by forceps. Shortening of the pipette was most crucial and had to be done as slowly and carefully as possible to avoid breaking the tip. Coating with Sylgard® helped to preserve the integrity of the tip. The silicon elastomer obviously damps high-frequent oscillations at the pipette tip. Finally, the solution at the back end of the short pipette was replaced by paraffin oil which reduced the risk of contaminating the pipette holder with solution (Benndorf, 1993).

Fig. 1 *A* illustrates a scanning electron micrograph of a typical pipette tip. The other pipette of the pair had a resistance of 63 MΩ (hypertonic solution). The ratio of the pore diameter to the outer diameter at the tip is approximately the same as in the glass material. The pore diameter was determined to be 190 nm. In general, pore diameters were found to be in the range of 170–210 nm ($n = 6$). The real pore diameters may be larger by up to 20 nm if the thickness of the gold layer (see Fig. 1, legend) at the internal rim equals that at the outside, though an estimate of the internal layer is certainly vague. Theoretically, the pore diameter d_t is related to the resistance R by (Sakmann and Neher, 1983)

$$R = \frac{4\rho l}{\pi d_s^2} + \frac{2\rho \cot(\varphi/2)}{\pi}\left(\frac{1}{d_t} - \frac{1}{d_s}\right) \tag{1}$$

with d_s being the internal diameter of the cylindrical shank, ρ the specific resistivity of the solution, φ the internal tip cone angle and l the length of the cylindrical shank. The first term of the sum is irrelevant for the further considerations because the silver wire was moved on to the beginning of the conical part. Assuming that the lumen of the whole conical part of the pipette approximates a single cone, $1/d_s$ is negligible with respect to $1/d_t$. R is therefore indirectly proportional to d_t. The specific resistivity ρ of the pipette solution was calculated to be 27.6 Ωcm (only Na^+, K^+, and Cl^- ions were considered; temperature = 25°C). The internal tip

angle φ was estimated to be 1.75° from the invariant outer angle of 7° of the conically shaped tip (measured from scanning electron micrographs; not shown) and the fairly constant ratio wall thickness/pore diameter. Eq. 1 then predicts for the 63 MΩ pipette, a pore diameter of 188 nm and a pore area of 0.028 μm^2 which is in line with the results of the scanning electron microscopy. In conclusion, patch pipettes as used in this study have pore areas of ~1/40 and less than that of typical hard glass pipettes with a resistance of 4 MΩ (Sakmann and Neher, 1983; corrected for different osmolarity of solutions). It should be stressed that the resistance of the high-ohmic pipettes used herein, if filled with *isotonic* solution, is nearly twice as high as indicated above.

Fig. 1 *B* shows an averaged trace from 40 consecutive traces as used to determine the seal resistance. To this aim, the filter was set to 1 kHz and the pulses were 500 ms long. Possible Na channel openings were not resolved at this bandwidth. The seal resistance was calculated from the late current to be 2 TΩ in this example.

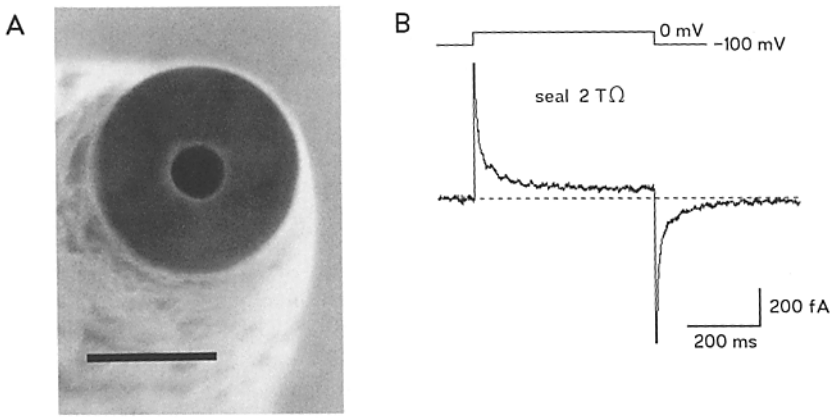

FIGURE 1. Patch pipettes used to form seals in the teraohm range. (*A*) Scanning electron micrograph of quasi tip-on view of a patch pipette. The resistance of the other pipette of the pair was 63 MΩ when filled with the hypertonic pipette solution. The pipette was vaporized with gold, such that all outer surface was expected to carry a final layer of ~10 nm. The pore diameter was determined to be ~190 nm (bar, 500 nm). (*B*) Teraohm seal. Pipette resistance 70 MΩ. The seal resistance was measured with 500-ms long voltage pulses from −100 to 0 mV; filter 1 kHz. The averaged current of 40 consecutive sweeps is shown. At the end of the pulse, the leak current amplitude is 50 fA resulting in a seal resistance of 2 TΩ.

Fig. 2 illustrates an amplitude histogram as used to calculate the rms noise level of the background noise at the band width of 20 kHz. Noise was measured before the subtraction of the 'sliding' averaged blank because this procedure artificially increases the rms noise in the corrected recordings by a factor of $(1 + 1/\sqrt{10})^{1/2} = 1.147$. The events are plotted on a logarithmic ordinate from a patch containing one active Na channel. The total interval of 450 ms results from 900 intervals of 500 μs duration each, which started 3.5 ms after the beginning of the test pulse and did not contain channel activity. Fitting the distribution with a Gaussian curve was used to determine its value to be 0.61 pA rms in this patch. Patches included in this study had a noise level of 0.59–0.71 pA rms.

Data Acquisition and Analysis

Recording and analysis of the data was performed on a PC-80486 with the ISO2 software developed in this lab (MFK Computer, Niedernhausen, Germany). All traces were recorded with the sampling rate of 100 kHz (12-bit resolution) and were stored on line on the hard disk and off line on an optical disk system.

Amplitude histograms of single-channel events with improved resolution were formed by the variance-mean technique as described by Patlak (1988). In brief, transition points were eliminated by shifting a window of a defined length along the traces, plotting the variance as function of mean current within the window, and discarding all original sampling points with variances above a defined threshold. The windows used here were 50 and 70 μs long at 20 and 8 kHz band width, respectively. The threshold variance was set to the variance of the background noise.

Because Na channels in mouse myocytes open at 25°C and above frequently with heterogeneous amplitudes (Benndorf, 1993), open times were evaluated from the distribution of additional gaps in the baseline noise (termed as baseline method henceforth). In the absence of noise, a hypothetical rectangular opening of original width t_w is after filtering (cut-off frequency

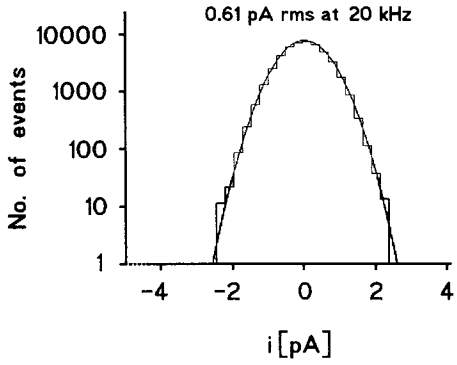

FIGURE 2. Noise in a teraohm seal at 20 kHz band width. Amplitude histogram of background noise on a logarithmic ordinate as formed from an interval of 450 ms. Holding potential −130 mV, pulse potential −40 mV. The histogram has been fitted with a Gaussian curve with a standard deviation (rms noise level) of 0.61 pA.

f_c) prolonged at the 10% level by approximately the rise time t_{10-90} if $t_w > t_{10-90}$. t_{10-90} is given by $0.3321/f_c$ (Colquhoun and Sigworth, 1983). At f_c = 20 kHz, t_{10-90} equals 16.6 μs. Background noise with an amplitude substantially larger than the 10% level also influences the open time. If the opening starts or ends just at the time when the noise is deflected in the direction of the channel openings it is prolonged. If it is deflected in the opposite direction it is shortened. Because long noise events are met by an opening statistically more often than short noise events, the mean prolongation must be some larger than $\bar{t}_n/2$ with $\bar{t}_n$ being the mean dwell time of the noise events. The mean shortening $\bar{t}_{sh}$ is even smaller being 4 μs at 20 kHz band width (Benndorf, 1994). Because all original openings exceeding t_{10-90} are prolonged on average by the same amount and if the fit starts only at the time $2\,t_{10-90} + \bar{t}_n/2 - t_{sh}$, the time constant of the distribution of the original openings and of the openings, evaluated at the 10% level, is equal. At multiple current amplitudes as frequently present in Na channels at elevated temperatures, a 10% level cannot be defined and it is therefore most useful to position the threshold in the center of the closed level. This leaves the validity of the previous considerations practically unaffected since the rms noise substantially exceeds the 10% level. Counting now all dwell times as events when the trace is below the midline of the closed level, results in a histogram composed of two distinct distributions. One is generated by the very large number of

dwell times t_n of noise events and the other by the smeared dwell times of opening events. The mean dwell time of noise events $\bar{t}_n$ for a Gaussian noise is given by (Papoulis, 1965)

$$\bar{t}_n = \frac{1}{2kf_c} \tag{2}$$

with k being a constant between 0.849 and 1.25, depending on the noise characteristic (Colquhoun and Sigworth, 1983). To separate the t_o- from the t_n-distribution, an exponential (time constant τ_n) can be fitted with high accuracy to the t_n-distribution if starting at the time $2t_{10-90} + \bar{t}_n/2 - t_{sh}$. τ_n was found to be very consistent.

Fig. 3 shows histograms of a file that contained 1,996 artificial openings which were distributed monoexponentially with a mean open time of 50 μs (amplitude 3.1 pA, noise 0.65 pA rms at 20 kHz). The histogram of the outwardly directed noise events (Fig. 3 *A*) was fitted monoexponentially with τ_n = 14 μs. Expansion of the ordinate (Fig. 3 *B*) illustrates that the fit was also reasonable for the rare longer events. The inset shows a trace with a 3.1 pA opening. The bars above indicate the time intervals which were included in the histogram, i.e., in this example only the noise events above the zero line were included, but not downwardly directed openings. This allowed to quantify the distribution of t_n independently of the opening events which is helpful to verify the position of the threshold in the middle of the baseline. Fig. 3, *C* and *D*, illustrates the respective histograms of the same file including only inwardly directed events. Reasonable fit of the histogram was possible with two exponentials, one with the time constant of the noise events (by reasons of symmetry it equals that of the outwardly directed events) and the other with the time constant of the openings. Expansion of the histogram (Fig. 3 *D*) illustrates the appropriateness of the fit to the longer opening events. As a result, τ_o of 51 μs estimated the original value very precisely.

Respective files with lower event amplitudes were generated to find a minimum event amplitude whose dwell time could be reliably analyzed. In other words, the limit was to find at which the frequency of noise events during the opening reaching the zero level causes notable event shortening. Given a noise of 0.61 pA rms and a mean open time of 50 μs, the threshold level was found empirically to be 1.3 pA for which the open time was determined to be 45 μs. This value was verified by calculating from the open time distribution with τ_o = 50 μs a respective modified open time histogram given that the average frequency of false events λ_f is (Papoulis, 1965)

$$\lambda_f = kf_c \exp\left(-\frac{\phi^2}{2\sigma^2}\right). \tag{3}$$

ϕ is the threshold and means here the event amplitude of 1.3 pA and σ is the rms noise. k and f_c have the same meaning as described above. The resulting histogram had more short and less long openings, because every ~500 μs, there is statistically one noise event exceeding 1.3 pA, thereby splitting one opening into two shorter openings. Fitting the resulting histogram yielded a mean open time of 44 μs, which agrees with the result found empirically. The level of 1.3 pA is therefore viewed to be approximately the threshold for a 10% error of the open time at noise levels typical in the measurements. Since the vast majority of Na channel openings were certainly larger than 1.3 pA, significant interference due to artificial closures is not likely in the data. Scatter of τ_o values in artificial files with an original mean open time of 50 μs and amplitudes larger than 1.3 pA was only within the narrow borders of 43 and 55 μs. In all patches, τ_n was verified by determining the respective value for the outwardly directed noise events; errors of only less than 3 μs were accepted. The main advantage of this method of evaluation of open times is that (*a*) it provides reliable results in the presence of heterogeneous

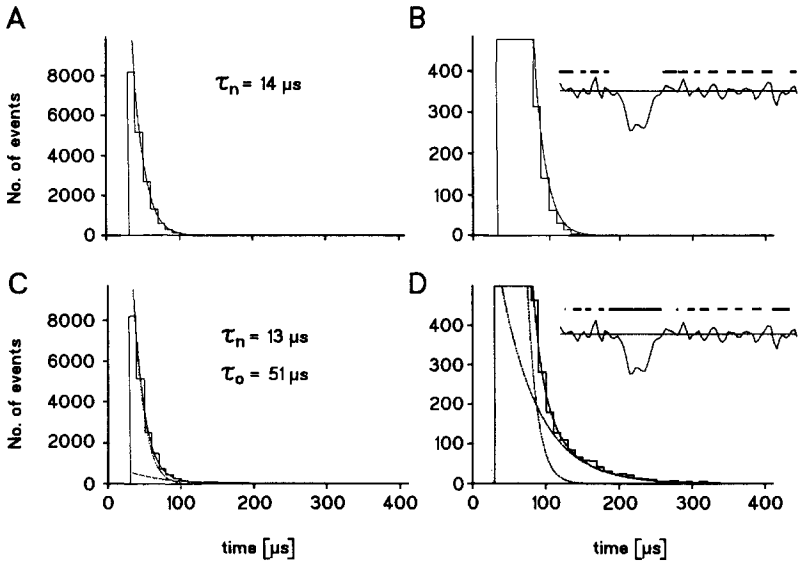

FIGURE 3. Baseline method to measure the open time of Na channels at 35°C. Files were created by superimposing noise from the recording system with exponentially distributed square pulses (mean duration 50 µs) delivered from a pulse generator. Cut-off frequency 20 kHz, 1996 traces of 4-ms duration, pulse amplitude 3.1 pA. Bin width of histograms 10 µs. (*A*) Setting the threshold of event detection to the midline of the closed level and evaluating the dwell times of the noise in the outward direction, provides, after clipping the first three bins, a monoexponential fit of the distribution with τ_n = 14 µs, independently of the openings. (*B*) Same diagram as in *A* at expanded ordinate. The curve also fits the rare longer noise events. (*Inset*) Trace with a long artificial opening. The bars above indicate the intervals included in the histogram. (*C*) Evaluation of the respective dwell times in the inward direction causes a histogram built by the overlap of two distributions, that of the noise events (τ_n) and that of the opening events (τ_o). (*D*) Expansion of the ordinate of the histogram in *C* illustrates that the distribution of the long events, here majorically caused by the artificial openings, is described well by the fit. The estimate of τ_o = 51 µs meets the mean of the original openings with high precision. The inset shows the same trace as in *B*. The bars indicate again the dwell times included in the histogram as generated by both the inwardly directed noise events *and* opening events.

levels and (*b*) it may be performed with noise levels double as high as any analysis employing the conventional 50% threshold.

RESULTS

Na Channels Open with Multiple Conductance States

Teraohm seals were obtained in 23 patches and they were often stable for 30 to 60 min, sometimes for 2 h. The noise regularly increased during this time by 5 to 10%. Six of these 23 patches contained activity of Na channels and five of these six patches

were viewed as patches containing *one and only one* channel (see Discussion). This study refers only to these five patches and they are denoted in the following patch 1 to patch 5. Fig. 4 illustrates single-channel currents and ensemble averaged currents (*top*) of a patch at three potentials formed from 1,000 consecutive sweeps each. In spite of opening the filter to 20 kHz, single-channel events could be easily recognized. As typical for voltage dependent Na channels, at the more depolarizing potentials, openings clustered at the beginning of the test pulse causing an ensemble

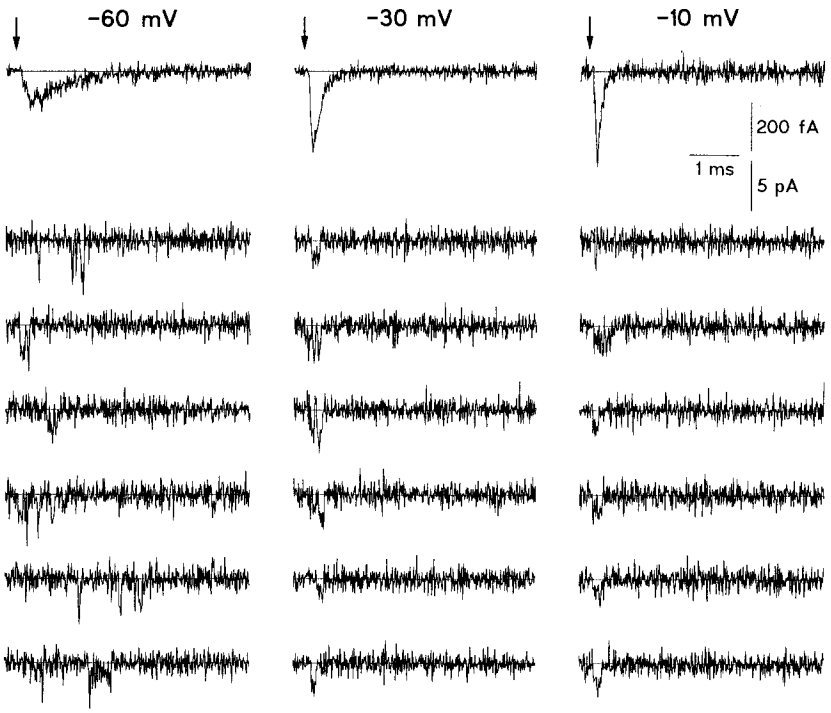

FIGURE 4. Single-channel and ensemble-averaged current traces of Na channels at 35°C at three potentials in patch 1. Band width, 20 kHz; holding potential, −140 mV; pulsing frequency, 20 Hz; sampling rate, 100 kHz; the arrows mark the beginning of the clamp pulse. The ensemble averaged currents were formed from 1,000 consecutive traces each. The openings are large and short and at more depolarizing potentials they cluster at the beginning of the clamp pulse.

averaged current which decayed at −10 mV completely within 300 μs. Inspection of the individual openings showed that the amplitudes were heterogeneous which is in line with the results at room temperature (Benndorf, 1993).

Fig. 5 *A* illustrates seven selected long openings ordered by magnitude in a patch containing one and only one channel. Within the resolution given by the noise, the channel could obviously open with all levels, between just detectable at ~1 pA and the largest at ~5 pA. In an attempt to resolve the relative contribution of individual levels, amplitude histograms were formed. At 20 kHz band width, amplitude

histograms including all sampling points showed only smeared distributions (Fig. 5 *B*) without any indication for the existence of preferential levels. To improve the resolution, amplitude histograms excluding transition points were formed by means of the variance-mean technique (Fig. 5 *C*). Included were intervals of only 50-μs duration with a threshold variance being that of the background noise. This means that each event in this type of histogram, deviating from the Gaussian curve fitted to the background noise events, corresponds to a true 50-μs interval of being open. The range of the largest levels varied among the patches between 4 and 5.5 pA and that of the most frequent levels between 2.5 and 3.8 pA (−50 mV). Similar smeared amplitude histograms were found in all patches. To further improve the resolution of the contributing levels, the traces were digitally filtered with a Gaussian algorithm

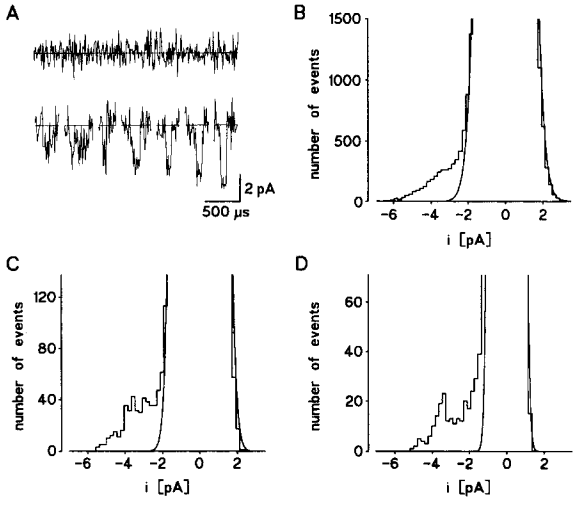

FIGURE 5. Heterogeneity of single-channel current amplitudes in patch 2. (*A, lower line*) selected long openings ordered by magnitude out of a file of 1,000 sweeps of one patch. Test potential −50 mV. The channel opened with multiple current levels. (*Upper line*) The baseline noise at 20-kHz band width. Holding potential −130 mV; test potential −50 mV. (*B*) Amplitude histogram including all sampling points calculated from all sweeps of the patch in *A*; f_c = 20 kHz. Here and in the following panels the distribution of the baseline noise events (*truncated*) was fitted with a Gaussian function (*curve*); SD = 0.721 pA. Histograms in *C* and *D* were formed from the same data as in *B*. (*C*) Amplitude histogram with improved resolution; window width and threshold in variance-mean analysis 50 μs and 0.520 pA², respectively; f_c = 20 kHz, SD = 0.542 pA. (*D*) Amplitude histogram with improved resolution at lower band width; window width and threshold in variance-mean analysis 70 μs and 0.115 pA², respectively; f_c = 8 kHz, SD = 0.316 pA.

and the window in the variance-mean technique was widened which means that only longer openings were included in the histogram. Reasonable histograms were obtained with the final cut-off frequency of 8 kHz and the window width of 70 μs. This combination of band width and window width occasionally resolved patterns in the distribution with events between 2.5 and 3.8 pA (−50 mV) being more frequent than smaller or larger events (Fig. 5 *D*).

In one of the single-channel patches, part of the events was approximately Gaussian distributed at four potentials which allowed to determine a conductance related to the mean of these distributions. Fig. 6 illustrates amplitude histograms with improved resolution. The more depolarizing potentials generated opening related peaks at smaller currents. These peaks were fitted with a Gaussian function and the

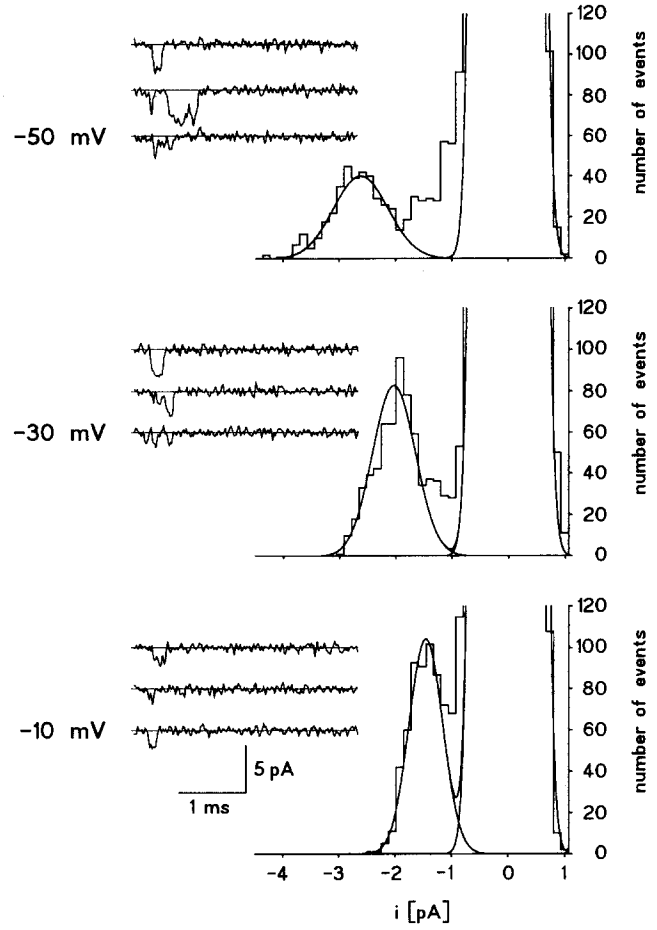

FIGURE 6. Amplitude histograms with improved resolution at three potentials formed from 1,000 consecutive sweeps each, patch 1. Holding potential −140 mV; f_c = 8 kHz, window width and threshold in variance-mean analysis 70 μs and 0.078 pA², respectively. The baseline noise events and part of the distribution of the opening-related events were fitted with Gaussian functions. The mean of the Gaussian curves fitted to the channel events at −50, −30, and −10 mV is −2.61, −2.02, and −1.45 pA, respectively. The SD values of both Gaussian curves at each potential are: −50 mV, 0.229 pA, 0.413 pA; −30 mV, 0.224 pA, 0.340 pA; −10 mV, 0.225 pA, and 0.297 pA. The traces show examples of openings at 8-kHz band width.

means of four such fits are plotted as function of voltage in Fig. 7 yielding the conductance of 27 pS. Compared with the opening events in the other patches, the openings in this patch seemed to be relatively small. Assuming the same reversal potential, the conductance related to the most frequent open level of 3.4 pA in Fig. 5 *D* would be, e.g., 37 pS. Interestingly, the standard deviation of Gaussian curves fitted to the opening related peaks in Fig. 6 decreased approximately proportional to the mean. If the possibility of an unresolved voltage-dependent flicker is ignored, such a dependence argues for the contribution of different levels to the opening

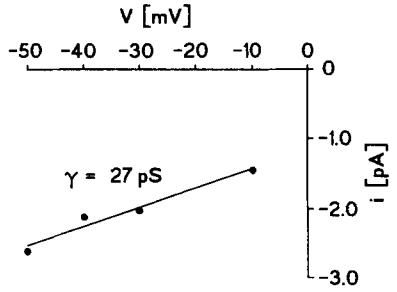

FIGURE 7. Current-voltage relationship for the approximately Gaussian distributed open level of patch 1 in Fig. 6. The mean of the fitted Gaussian curve has been plotted. The slope conductance [g]g was calculated by linear regression.

related peak because the shot noise and the Johnson noise generated by the open channel would increase the total rms noise by only less than 10% (see Discussion).

Fig. 8 illustrates selected traces with complex opening patterns at two band widths (20 kHz left, 8 kHz right). These traces further support that the same channel may generate different level openings, including large ones, and also that it may switch directly *between* different levels. Fig. 8 *A* shows a sequence of four complete events, containing an opening and a closing transition each. This indicates that an Na channel may repeatedly switch within 1 ms from a closed state to multiple open states. The traces in Fig. 8 *B* resolve at 8 kHz a sojourn at an intermediate level which has been reached from and left for a larger level, i.e., a channel may directly switch between different open states. The burst of four openings with peak sampling points between 4.5 and 5.5 pA demonstrated in Fig. 8 *C* contained three direct transitions from the closed to the open level and four direct transitions in the reverse direction. During the third opening transition, the 8 kHz-filtered trace suggests that a smaller level has been passed (*arrow*). The sequence of openings in Fig. 8 *C* (*left*) supports that these large openings were generated by the action of only one channel because it is extremely unlikely that two independent channels would have switched seven times synchroneously.

The heterogeneity of the levels generally questions any simple evaluation of the peak open probability P_o (the open probability at the peak of the ensemble averaged current), either for the largest observed levels, the most frequent levels, or any other

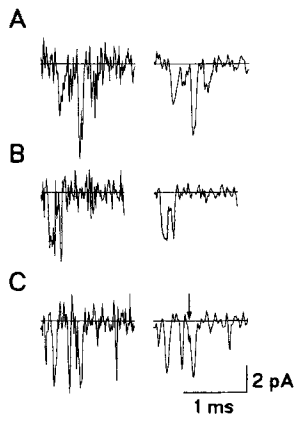

FIGURE 8. Na channels switch between different conductance states, patch 3. Holding potential −130 mV; test potential −50 mV. Each trace is shown at two band widths, at 20 kHz (*left*) and after off-line filtering with a Gaussian algorithm at a final frequency of 8 kHz. (*A*) Burst with heterogeneous openings. After the first opening the channel changed its conductance three times within 1 ms. (*B*) Evaluated at 8-kHz band width, a lower conductance state was reached from a larger level and was finished by transiting again to a larger level. (*C*) Four large, spike-like openings with one of the eight transitions possibly passing a lower level (*arrow*).

intermediate levels. For comparison with previous results, P_o has been calculated for the Gaussian-like distributed level of patch 1 to be at −50, −30, −10, and −40 mV (in the sequence of their recording) 0.14, 0.15, 0.26, and 0.04, respectively. If related to any larger levels, these probabilities would be correspondingly smaller. From the first three values it is obvious that P_o increases at more depolarizing potentials, however to a lesser degree than expected from experiments in macroscopic currents. Surprisingly, the last P_o value at −40 mV is only 30% of that at −50 mV. This does not fit to data in macroscopic currents and indicates that P_o in single-channel experiments is also a function of time thereby further complicating its evaluation.

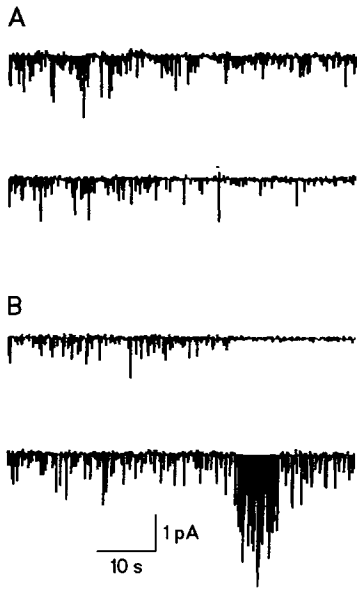

FIGURE 9. Time courses of the Na channel activity over a period of 50 s. The ensemble averaged current in the first two ms of a test pulse to depolarizing potentials (V_t) has been calculated and plotted as vertical line to the zero line, i.e., a downwardly directed line is longer in proportion to the duration, the amplitude, and the number of openings within the 2-ms interval. Pulsing frequency 20 Hz. (*A, top*) Stationary channel activity in the range of tens of seconds with clusters in the range of seconds, V_t = −50 mV, patch 1. (*Bottom*) Decreasing channel activity, V_t = −40 mV, patch 4. (*B*) Examples of data files with abrupt changes of channel activity. (*Top*) Channel activity was switched off 33 s after the beginning of the interval, V_t = −30 mV, patch 4. (*Bottom*) Switch for 6 s to mode 2 openings (no inactivation, dramatically increased mean open time), V_t = −50 mV, patch 2. Periods of mode 2 openings were excluded in any statistical analysis.

The Action of Individual Na Channels Is Time Dependent

Fig. 9 illustrates time courses of the mean current over a period of 50 s which corresponds to 1,000 sweeps. Evaluated were the first 2 ms of the individual traces. Examples of files with a stationary or slowly changing action of a Na channel are demonstrated in Fig. 9 *A*. The upper time course was of the most frequent type: though the channel action was grouped to clusters in the range of seconds, the averaged action in the range of tens of seconds was fairly stationary. The lower time course illustrates another patch. The channel activity was present during the whole illustrated period but clearly decreased in time. Examples of files with sudden dramatic changes of the action of a Na channel are demonstrated in Fig. 9 *B*. The upper time course shows a trace with typical channel activity during the first 33 s. After this time the activity of the channel was completely lost. With respect to the stationarity of the Na channel action, inspection of long time courses of all available

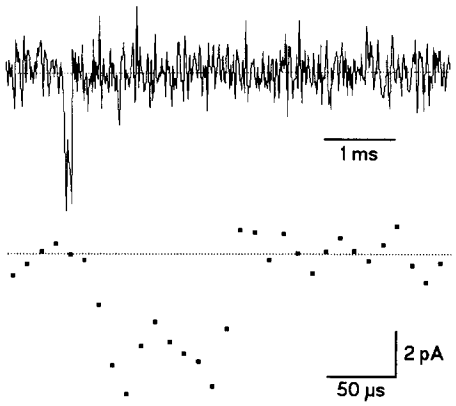

FIGURE 10. Risetime of an Na channel opening at 20 kHz band width, patch 2. The top trace illustrates an opening of an Na channel, as elicited when clamping from −130 mV to the test potential of −50 mV. Plotting only the sampling points of the opening (sampling interval 10 µs) at increased time resolution shows that the transition times are in the order of the theoretical rise time of 16.6 µs.

data did not show obvious potential-dependent differences. The lower time course shows usual channel activity during the first 30 s. Then P_o was switched for 6 s to dramatically higher values. Beside the larger P_o, these opening events differed substantially from the usual openings by a predominant amplitude (3.8 pA at −50 mV), a mean open time in the range of 200 µs and a complete loss of inactivation. In all recordings, such a switch of P_o was found only a second time in a short interval of 0.5 s. Intervals with this type of openings, which correspond most likely to the mode 2 openings of Na channels reported by Patlak and Ortiz (1986, 1989), were excluded in all statistical analysis.

At 35°C Na Channel Open Time Is in the Range of Several Tens of Microseconds

Before evaluating the open times of the short events, it was tested whether 20 kHz passed the recording system. To this aim, the rise time t_{10-90} of the most rapid transitions of the channel events was evaluated under the assumption that these transitions were generated by instantaneous openings. Fig. 10 illustrates a trace containing a long opening of an Na channel. Plotting only the sampling points at

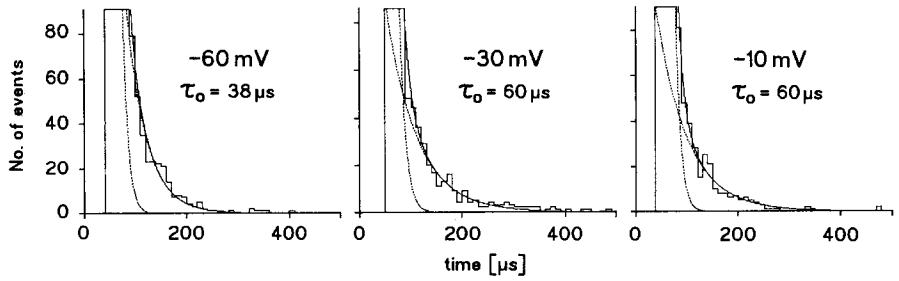

FIGURE 11. Mean open time of single Na channels at 35°C as measured with the baseline method (see Methods) at three voltages. The histograms were formed from 1,000 consecutive traces each. Holding potential, −140 mV; bin width 10 µs, patch 1. The opening related distributions could be separated well from the noise distributions yeilding the mean open times τ_o as indicated. τ_n was determined to be 14, 15, and 13 µs at −60, −30, and −10 mV, respectively.

increased time resolution shows that both the opening and the closing transition take place in a time scale similar to the theoretical value. It is therefore concluded that only the filter with f_c = 20 kHz limits the recording band width, i.e., true openings longer than t_{10-90} = 16.6 μs would reach approximately the full amplitude (Colquhoun and Sigworth, 1983).

Fig. 11 shows open time histograms which have been formed with the baseline method at three voltages. The opening event distributions could be clearly separated from the noise event distributions and could be fitted reasonably well with single exponentials with the indicated time constants. The mean open time increased at less negative potentials. Very few longer events at −30 mV and −10 mV deviate from the theoretical curve. These exceptional openings might indicate that the channel has switched for short time intervals to a different open state, e.g., mode 2, which could have been too short to be recognized by the inspection of the time courses as shown in Fig. 9. Fig. 12 summarizes the results obtained in five patches containing activity of

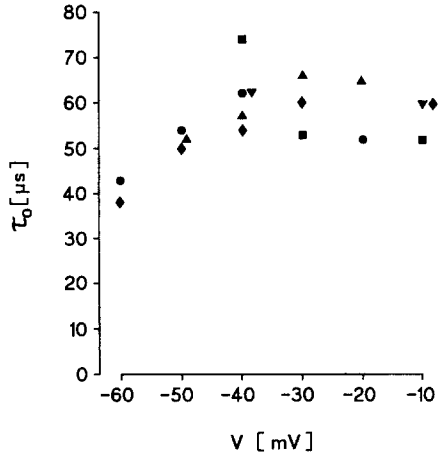

FIGURE 12. Mean open time τ_o as function of voltage. The symbols correspond to the following patches: ◆, patch 1, ●, patch 2, ▼, patch 3, ■, patch 4, ▲, patch 5. All data points were calculated with the baseline method from between 740 and 2,000 traces.

only one channel. In all patches the mean open time was between 38 and 74 μs, the averaged standard deviation of τ_o at all potentials was 17 μs if the exceptionally long openings were excluded. The mean open time at −60 mV was significantly shorter than at the other voltages between −50 and −10 mV. In the direction of the most depolarized potentials, however, τ_o did not significantly decrease as found at lower temperature (Yue et al., 1989; Benndorf and Koopmann, 1993).

DISCUSSION

The main results of this report are (*a*) Low noise single-channel recordings were performed by using thick-walled pipettes with small pore diameters (~200 nm). The noise was sufficiently low to study properties of voltage-dependent Na channels at 35°C at a band width of 20 kHz. (*b*) Only 6 out of 23 such patches contained functional Na channels. This low incidence increased the chance to study one and only one channel. (*c*) The amplitude of the single Na channel currents was

heterogeneous and its distribution generally varied considerably. In one patch, the open probability was determined at different voltages for an approximately Gaussian distributed level to be 0.26 at −10 mV. (*d*) The mean open time of the heterogeneous Na channel openings was measured from the distribution of the opening-related gaps in the middle of the noisy baseline to be between 38 and 74 μs.

Low Noise Recording with Small-Pore Patch Pipettes

In comparison with previous studies, where the same pipette holder in combination with short pipettes of only 5–20 MΩ was used (Benndorf, 1993; Benndorf and Koopmann, 1993), noise could be further reduced from a minimal value of 0.145 to 0.109 pA rms (f_c = 5 kHz). This reduction of noise allowed to increase the recording band width to 20 kHz. One reason for the low noise performance was the thick wall of the pipettes which considerably reduces the pipette capacitance and thereby the pipette *RC* noise which is the leading noise source in the high-ohmic pipettes used here. Another reason was the smaller pore diameter which enabled seal resistances of several TΩ thereby reducing the Johnson noise and the shot noise in the patch/seal combination to negligible values (see also Benndorf, 1994). The seal resistance with the small-pore pipettes was also very stable which was a prerequisite for using the baseline method to measure the mean channel open time.

An even lower noise level was reported recently by Levis and Rae (1993) using quartz pipettes, an amplifier with an electronic noise of only 0.048 pA rms, and excessive Sylgard® coating. The strategy to minimize noise described here has the advantage that borosilicate glass and ordinary pullers can be used. The noise difference between the two techniques (typical values 0.120 to 0.085 pA rms at f_c = 5 kHz) is even smaller with respect to the different pipettes if the improved amplifier of Levis and Rae (1993) (0.048 compared to 0.068 pA rms at f_c = 5 kHz) is taken into consideration. Furthermore, at higher band widths, reducing the pipette capacitance by increasing the wall thickness and more extensive coating with Sylgard® is more effective in reducing noise than using tubing material with low dielectric loss. This is because measured power spectra increase in proportion to f^2 whereas the power spectrum of dielectric noise increases only proportional to f (for more details see Benndorf, 1994).

The Heterogeneous Levels and the Open Probability

A further reason to work with pipettes with exceptionally small pore diameters was to increase the incidence to have *one and only one* active Na channel in the patch. With the assumption of a statistical distribution of the channels in the membrane, the ratio of six patches containing channel activity to a total of 23 patches allowed a rough evaluation of the probability P_1 to have a patch containing only *one* channel. If P_1^m is the probability to have m active channels in the patch, then the relation,

$$P_1 + P_1^2 + P_1^3 + \cdots = 6/23, \tag{4}$$

holds. Using the identity $\Sigma_{m=1}^{\infty} P_1^m = P_1/(1 - P_1)$, for $|P_1| < 1$, yields $P_1 = 0.21$ and the summed probability of 0.05 to have more than one active channel. This means that it is about four times more likely to have a patch with activity of only one channel

than of multiple channels. This agrees well with the ratio found in this study that five of the six patches with channel activity did not show any indication to contain more than one channel. Only one patch produced an ensemble averaged current more than twice as large as the largest in the other five patches and also developed the largest events; the maximum sampling point at −50 mV was 7.5 pA. This patch was therefore considered to contain two channels and was excluded from the statistical analysis. It should be noted that the short open times, the large background noise at 20 kHz band width, and the heterogenous amplitudes did not allow to decide unequivocally for more complex events whether one channel or two channels were present. Support to have only one channel in a patch came from the high incidence of rapid transitions between large open levels and the closed level in the range of the rise time t_{10-90} (Fig. 8 *C*) because it is not likely that these large events were generated by the simultaneous action of two independent channels.

The fact that the standard deviation of the Gaussian-like distribution of part of the open levels in Fig. 6 clearly exceeds that in the baseline noise, raises the question to what extent it is related to the variability among the levels themselves. This question may be addressed by estimating the contribution of other noise sources generated by the open channel, as Johnson and shot noise which may be calculated directly (Hamill et al., 1981). Assuming for the open channel a resistance of 2.5×10^{10} Ω, the variance of the Johnson noise is calculated to be 5.26×10^{-27} A^2 and with a single-channel current of 4 and 2 pA at −50 and −10 mV, the shot noise variance is calculated to be 1.0×10^{-26} A^2 and 0.51×10^{-26} A^2, respectively, (f_c = 8 kHz). If these both noise types add to the background noise of 7.81×10^{-26} A^2 (this is the noise in the traces and not that determined in Fig. 6 after using the variance-mean technique) the standard deviation would increase by only 9.5 and 6% at −50 and −10 mV, respectively. If the possibility of an unresolved voltage-dependent flicker is ignored, it is concluded that the larger standard deviation in the Gaussian-like distribution of part of the open levels than that in the baseline noise is mainly due to different levels themselves. Furthermore, the ratio of the standard deviations of the Gaussian curves in the opening peak and the baseline noise peak at −50 mV is 1.80 and this is larger than the value of 1.41 calculated from a corresponding histogramm at 24°C (Fig. 6 *A*, *right*, in Benndorf, 1993). Under the assumption that both experiments are comparable, this supports the idea that the degree of heterogeneity increases at the higher temperature. (The temperature coefficient Q_{10} of the mean of the Gaussian-like distributed open level would be 1.16.) Openings of Na channels larger than usual openings were also reported after treatment of cardiac cells with lysophosphatidylcholine (LPC; Undrovinas, Fleidervish, and Makielski, 1992). At the present it is not clear whether there is a relation of the largest levels found here and these LPC induced openings. It is attractive, however, to speculate that a surplus of LPC only stabilizes a state which a channel may also reach under normal conditions since LPC is a constituent of the membrane.

The estimated values of the peak P_o in one patch are certainly vague and it is stressed again that these values correspond to an approximately Gaussian distributed level in a histogram, which clearly contained also levels deviating from the theoretical curve. If related to a larger level, which might be the fully open level, the P_o values would be correspondingly smaller. If smaller levels contributed to a larger degree to

the mean current (−50 mV in Fig. 6), the present analysis certainly underestimated P_o. Slight underestimation of P_o might be possible due to an incomplete recovery from a slow inactivation process during the interpulses of 46 ms after the test pulses of 4 ms. The degree of slow inactivation, however, is expected to be very small because (*a*) the recovery time is 12.5 times longer than the time for the onset of slow inactivation and (*b*) slow inactivation recovers rapidly already at −120 mV and room temperature (τ = 11 ms; Benndorf and Nilius, 1987). The maximum P_o value of 0.26 found at −10 mV is in the order of some of the previous results (0.3 by Aldrich, Corey, and Stevens, 1983; 0.4 by Benndorf, 1988). Other investigators reported substantially larger values (0.6 by Horn and Vandenberg, 1984, and by Kimitsuki, Mitsuiye, and Noma, 1990*a*). The present analysis of P_o also showed that the action of Na channels is in general not stationary (Fig. 9). Although neither the mechanisms underlying the changes in the activity of the channels nor the incidence of their appearance are understood at the present, one may speculate that such changes may be the reason for the variability found for P_o. Study of the open probability in Na channels should therefore deliver more consistent results, if the analysis refers to comparable phases in long time courses as shown in Fig. 9. Apparently larger values may, of course, also be obtained if the channel number in the patch is underestimated. In this respect, measurements with the tipped pipettes used here are certainly superior.

In general, voltage dependent gating of Na channels seems to be more affected by the small-pore pipettes than by conventional pipettes. A shift of steady state inactivation to negative potentials by more than 30 mV (Kimitsuki, Mitsuiye, and Noma, 1990*b*) was possible and this shift was sometimes time dependent. Therefore, the holding potential was set to sufficiently negative potentials where any inactivation was obviously absent. Reasons for these alterations might be the smaller radius of the curvature of the patch or the shorter distance of the channel in the patch to the surrounding glass. Despite the obviously more severe and frequent alterations of Na channels, there were also patches which were not altered more than found with conventional patch pipettes, i.e., cardiac Na channels may work in these tiny patches very similar as in patches of conventional size.

The Baseline Method for Evaluation of the Mean Open Time

The technique to determine the mean open time of a channel in the center of the baseline noise yielded surprisingly consistent results among the patches. The consistency of the results was superior to all types of threshold setting in the range of half maximum amplitudes, even in selected openings of approximately uniform amplitude. One advantage of the method is that the noise in the recordings can be substantially larger which allowed to increase the recording band width thereby including shorter events in the analysis. Because at elevated band width, the noise events t_n were also shortened and their distribution could be fitted with high accuracy with a single exponential yielding the time constant τ_n, τ_o could be separated from τ_n reasonably well if τ_o was at least two times larger than τ_n. A second advantage of the method is that it may be easily used in channels which open with heterogeneous levels, as found here at 35°C in Na channels. Theoretically, if the baseline method and the 50% threshold method are applied to the same, equally filtered records, the

mean open time, determined with the baseline method, must be longer because the baseline method ignores that part of the short closing events, which have been too short to reach the baseline, but have crossed the 50% level. However, since the baseline method allows analysis of records in the presence of about double the background noise tolerable with the 50% level technique, the recording band width may be increased. For a more thorough discussion of this method see Benndorf (1994).

Mean Open Time of Na Channels at 35°C

Determination of the temperature coefficient Q_{10} has allowed in the past to extrapolate open times determined at lower temperatures to higher temperatures. A prerequisite for such an extrapolation was that the temperature coefficient itself is *independent* of the temperature. For the mean open time of Na channels in the guinea pig myocardium, a Q_{10} of 2.1 has been reported by Kimitsuki et al. (1990*a*). Based on measurements at 10 and 25°C, Benndorf and Koopmann (1993) have reported recently that the Q_{10} value in Na channels of the mouse myocardium was considerably larger than 2.1 and, furthermore, also *voltage dependent:* At −50 mV, Q_{10} was found to be as large as 4.8 whereas at 0 mV a value of 3.6 was determined. From this voltage-dependent temperature sensitivity of the mean open time, different entropy changes associated with deactivation and inactivation were calculated. From the present data at 35°C and the values at 25°C in the previous study, a Q_{10} value of ~3 calculates for the potentials between −40 and −10 mV. The most reasonable explanation of the larger Q_{10} of 3 compared to the value of 2.1 of Kimitsuki et al. (1990*a*) is certainly the improved resolution in the present study.

At 35°C τ_o was obviously voltage independent at the more depolarized potentials (Fig. 10) which differs from data at 25°C (Benndorf and Koopmann, 1993). In terms of rate constants this implies that the rate constant of microscopic inactivation, determining the transition from the open to the inactivated state (Aldrich et al., 1983), is voltage independent at elevated temperature. If fast inactivation of a channel takes place by binding of an intracellular loop between domains III and IV to a receptor (Vassilev, Scheurer, and Catterall, 1988), such a loss of voltage dependence might indicate that a voltage-independent step becomes rate limiting at the higher temperature which might, e.g., be the diffusional movement of the loop. Another possible explanation for such a loss of voltage dependence of inactivation at the higher temperature is a phase transition in the phospholipid matrix (Schwarz, 1979) which would affect preferably arrangements in the channel molecule associated with inactivation.

Kinetic analysis has been performed exclusively in recordings which did not show slow time-dependent increase of τ_o or loss of inactivation. Also the contemporary loss of inactivation during periods of noninactivating bursts (mode-2 openings; Patlak and Ortiz, 1986, 1989) was excluded from the kinetic analysis, because openings in such periods of seconds to tens of seconds were frequent and therefore prolonged the mean open time dramatically. To my impression, occasional irreversible steady increase of τ_o and reversible switch to mode 2 were caused by different mechanisms not only because of their different way of occurrence; mode-2 openings appeared in long bursts, i.e., there was frequent reopening whereas steady τ_o prolongation left the

number of openings fairly unaffected. In the ensemble averaged currents of 4-ms duration, mode-2 openings caused a complete loss of inactivation whereas the steady increase of τ_o implied only a steady increase of the time constant of macroscopic inactivation. Only in extreme cases, macroscopic time courses could not be distinguished. Analysis of more data would be necessary to precisely quantify and distinguish both phenomena.

I thank H.-P. Bollhagen and M. Langenkamp for the help with the scanning electron microscopy, T. Böhle and B. Doepner for carefully reading the manuscript, and D. Metzler and R. Kemkes for excellent technical assistance.

This study was supported by the grant Be 1250/4-1 of the Deutsche Forschungsgemeinschaft. K. Benndorf is a Heisenberg fellow of the Deutsche Forschungsgemeinschaft.

Original version received 30 April 1993 and accepted version received 21 July 1994.

REFERENCES

Aldrich, R. W., D. P. Corey, and C. F. Stevens. 1983. A reinterpretation of mammalian sodium channel gating based on single channel recording. *Nature.* 306:436–441.

Benndorf, K. 1988. Patch clamp analysis of Na channel gating in mammalian myocardium: reconstruction of double pulse inactivation and voltage dependence of Na currents. *General Physiology and Biophysics.* 7:353–378.

Benndorf, K. 1993. Multiple levels of native cardiac Na^+ channels at elevated temperature measured with high-bandwidth/low-noise patch clamp. *Pflügers Archiv.* 422:506–515.

Benndorf, K. 1994. Low noise recording. *In* Single Channel Recording. Second edition. B. Sakmann and E. Neher, editors. Plenum Publishing Corp., New York. In press.

Benndorf, K., W. Boldt, and B. Nilius. 1985. Sodium current in single myocardial mouse cells. *Pflügers Archiv.* 404:190–196.

Benndorf, K., and R. Koopmann. 1993. Thermodynamic entropy of two distinct conformational transitions of single ionic channel molecules. *Biophysical Journal.* 65:1585–1589.

Benndorf, K., and B. Nilius. 1987. Inactivation of sodium channels in isolated myocardial mouse cells. *European Biophysics Journal.* 15:117–127.

Brown, A. M., K. S. Lee, and T. Powell. 1981. Sodium current in single rat heart muscle cells. *Journal of Physiology.* 318:479–500.

Bustamante, O. 1983. Sodium currents in segments of human heart cells. *Science.* 220:320–321.

Cachelin, A. B., J. E. DePeyer, S. Kokubun, and H. Reuter. 1983. Sodium channels in cultured cardiac cells. *Journal of Physiology.* 340:389–401.

Colquhoun, D., and F. Sigworth. 1983. *In* Single Channel Recording. First edition. B. Sakmann and E. Neher, editors. Plenum Publishing Corp., New York. 191–263.

Ebihara, L., N. Shigeto, M. Lieberman, and E. A. Johnson. 1980. The initial inward current in spherical clusters of chick embryonic heart cells. *Journal of General Physiology.* 75:437–456.

Hamill, O. P., A. Marty, E. Neher, B. Sakmann, and F. J. Sigworth. 1981. Improved patch-clamp technique for high-resolution current recording from cells and cell-free membrane patches. *Pflügers Archiv.* 391:85–100.

Horn, R., and C. A. Vandenberg. 1984. Statistical properties of single sodium channels. *Journal of General Physiology.* 84:505–534.

Kimitsuki, T., T. Mitsuiye, and A. Noma. 1990*a*. Maximum open probability of single Na^+ channels during depolarization in guinea-pig cardiac cells. *Pflügers Archiv.* 416:493–500.

Kimitsuki, T., T. Mitsuiye, and A. Noma. 1990*b*. Negative shift of cardiac Na^+ channel kinetics in cell-attached patch recordings. *American Journal of Physiology*. 258:H247–254.

Kunze, D. L., A. E. Lacerda, D. L. Wilson, and A. M. Brown. 1985. Cardiac Na currents and the inactivating, reopening, and waiting properties of single cardiac Na channels. *Journal of General Physiology*. 86:691–719.

Lee, K. S., T. A. Weeks, R. L. Kao, N. Akaike, and A. M. Brown. 1979. Sodium current in single rat heart muscle cells. *Nature*. 278:269–271.

Levis, R. A., and J. L. Rae. 1993. The use of quartz patch pipettes for low noise single channel recording. *Biophysical Journal* 65:1666–1677.

Murray, K. T., A. Takafumi, P. B. Bennett, and L. M. Hondeghem. 1990. Voltage clamp of the cardiac sodium current at 37°C in physiologic solutions. *Biophysical Journal*. 57:607–613.

Papoulis, A. 1991. Probability, Random Variables and Stochastic Processes. McGraw Hill, New York. 603–612.

Patlak, J. B. 1988. Sodium current subconductance levels measured with a new variance-mean analysis. *Journal of General Physiology*. 92:413–430.

Patlak, J., and M. J. Ortiz. 1986. Two modes of gating during late Na^+ channel currents in frog sartorius muscle. *Journal of General Physiology*. 87:305–326.

Patlak, J., and M. J. Ortiz. 1989. Kinetic diversity of Na^+ channel bursts in frog skeletal muscle. *Journal of General Physiology*. 94:279–301.

Pröbstle, T., R. Rüdel, and J. P. Ruppersberg. 1988. Hodgkin-Huxley parameters of the sodium channels in human myoballs. *Pflügers Archiv*. 412:264–269.

Sakmann, B., and E. Neher. 1983. *In* Single Channel Recording. B. Sakmann and E. Neher, editors. Plenum Publishing Corp., NY. 37–51.

Scanley, B. E., and H. A. Fozzard. 1987. Low conductance sodium channels in canine cardiac Purkinje cells. *Biophysical Journal*. 52:489–495.

Schwarz, W. 1979. Temperature experiments on nerve and muscle membranes of frogs. Indications for a phase transition. *Pflügers Archiv*. 382:27–34.

Undrovinas, A. I., I. A. Fleidervish, and J. C. Makielski. 1992. Inward sodium current at resting potentials in single cardiac myocytes induced by the ischemic metabolite lysophosphatidylcholine. *Circulation Research*. 71:1231–1241.

Vandenberg, C. A., and R. Horn. 1984. Inactivation viewed through single sodium channels. *Journal of General Physiology*. 84:535–564.

Vassilev, P. M., T. Scheurer, and W. A. Catterall. 1988. Identification of an intracellular peptide segment involved in sodium channel inactivation. *Science*. 241:1658–1661.

Yue, D. T., J. H. Lawrence, and E. Marban. 1989. Two molecular transitions influence cardiac sodium channel gating. *Science*. 244:349–352.